Original research article

Planar positioning bias due to transmitter and receiver tilting in RSS-based ranging VLP

Nobby Stevens[a,*], Heidi Steendam[b]

[a] *KU Leuven, ESAT-DRAMCO, Ghent Technology Campus, Ghent, Belgium*
[b] *Ghent University, TELIN/IMEC, Ghent, Belgium*

A R T I C L E   I N F O

A B S T R A C T

In this work, a set of general expressions treating both transmitter and receiver tilt in received signal strength based visible light positioning is elaborated. A meticulous approach involving Euler rotations leads to a compact expression for the modified channel gain that can be interpreted graphically. It is demonstrated that ignoring even small tilt angles can easily result in a bias of the planar positioning estimation in the order of several tens of centimeters in realistic settings. As a result, it is important to take into account the receiver and transmitter tilt for obtaining highly accurate indoor localization by means of received signal strength based visible light positioning. Based on the modified channel gain, a simple and accurate rule-of-thumb is formulated, allowing to determine the worst-case planar position errors when tilting angles are ignored.

1. Introduction

The topic of accurate indoor positioning has been investigated for several decades [1]. Multiple signals of different nature are hereby analysed. A majority of the research efforts can be found in the usage of ubiquitous radio frequency (RF) signals emitted by WiFi, Bluetooth or other RF communication technologies [2]. More recently though, a technique based on the modulation of artificial visible light has emerged, exploiting the omnipresence of indoor illumination infrastructures [3,4]. Several papers on the potential accuracies [5–8] and multiple access techniques [9] of this novel technique, called Visible Light Positioning (VLP), have been published. In a large majority of these publications, the signal transmitting light emitting diode (LED) is pointing perfectly downwards while the receiving photo diode (PD) is oriented upwards. In reality though, one can imagine that this situation is more an exception than a rule. Regarding the LED, attachment of this device at the ceiling or on a dedicated rail can easily introduce a small tilt due to the mechanical fixation. Recent work [10] has studied the impact of transmitter tilt on the position estimation, where tilt angles of 1 and 2 degrees were considered. At the receiver side, the time-varying presence of small tilts is obvious, even if the PD is attached on the roof of e.g., a forklift truck. When the vehicle is charged with a large weight, one can imagine that the roof becomes tilted towards the increased weight lifted by the arms of the truck. In [11], error compensation for receiver tilt was considered. The particular application scenario that needs highly accurate positioning is the localization of autonomous guided vehicles (AGV) in indoor premises. Considering the width of the corridors in warehouses and the observation that multiple AGVs maneuver in these premises, an accuracy of sub 10 cm is needed.

In previous work, the tilting impact on the channel gain in received signal strength (RSS) ranging-based VLP was quantified [12].

* Corresponding author.
  E-mail address: nobby.stevens@kuleuven.be (N. Stevens).

Here, the impact on the planar position estimation bias in the presence of both transmitter and receiver tilt is evaluated. In Section 2, the modification of the channel gain is elaborated. In Section 3, the planar distance estimation under tilting conditions is analysed and numerically evaluated. A closed-form expression for the planar position is found. Multiple representative configurations are studied, including tilting of the receiver and transmitter, leading to a positioning error value when these tilt angles are not taken into account. This has led to a simple and generally applicable rule-of-thumb for the maximum mean absolute error.

2. System description

To determine the distance between an LED and the PD, we evaluate the RSS. The RSS signal at the PD output is given as [6]

$$r(t) = R_p \alpha s(t) + n(t), \tag{1}$$

where R_p is the responsivity of the PD, α the channel gain, $s(t)$ the transmitted optical power signal during a time slot with duration T_s and $n(t)$ the additive noise contribution. This noise is typically modelled as zero-mean Gaussian noise with power spectral density N_0. From the received signal, we extract an RSS value, by correlating $r(t)$ with $s(t)$ in the interval $[0, T_s]$. Assuming perfect synchronization, the RSS value yields

$$r = R_p \alpha P_s + n, \tag{2}$$

where $P_s = \int_0^{T_s} s^2(t)dt$, and the noise term $n = \int_0^{T_s} s(t)n(t)dt$ is zero-mean Gaussian noise with variance $N_0 P_s$. In this work, we will not include the noise contribution since the focus is on the modification of the channel gain and planar distance estimation when the transmitter and receiver are tilted. The observation that the precision deterioration due to noise of the position estimation is very limited [13,14] further motivates this choice. In (2), the channel gain when the receiver is in line-of-sight of the transmitter without any other contribution (e.g., reflections by walls) can be written as

$$\alpha = \frac{(m+1)A}{2\pi d^2} \cos^m \phi_S \cos \phi_R T(\phi_R) g(\phi_R), \tag{3}$$

where A is the surface of the PD, m is the Lambertian order of the LED, d is the Euclidian distance between the LED and the PD, $T(\phi_R)$ is the signal transmission gain, and $g(\phi_R)$ the concentrator gain [15]. Further, the angles ϕ_S and ϕ_R correspond to the angle of radiation and the angle of incidence, respectively and are defined as in Fig. 1; $\cos \phi_S$ and $\cos \phi_R$ are found by

$$\cos \phi_S = \mathbf{n}_S \cdot \frac{\mathbf{r}_R - \mathbf{r}_S}{d} \tag{4}$$

$$\cos \phi_R = \mathbf{n}_R \cdot \frac{\mathbf{r}_S - \mathbf{r}_R}{d} \tag{5}$$

where $\mathbf{n}_S$ and $\mathbf{n}_R$ are the unit normal vectors of the LED and photo diode. In Fig. 1, the global coordinate system (GCS) that is linked to the room is introduced. The vectors $\mathbf{r}_S$ and $\mathbf{r}_R$ are the location vectors of respectively the transmitting LED and receiving PD. In (3), the concentrator gain can be written as
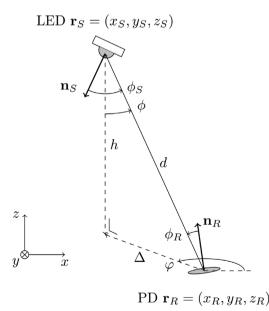

Fig. 1. The transmitting LED is situated at $\mathbf{r}_S = (x_S, y_S, z_S)$, while the receiving photodiode at $\mathbf{r}_R = (x_R, y_R, z_R)$.

$$g(\phi_R) = \begin{cases} \dfrac{n_c^2}{\cos^2 \psi_c} & 0 \le \phi_R \le \psi_c, \\ 0 & \phi_R > \psi_c \end{cases}$$

(6)

where n_c is the refractive index of the concentrator, and ψ_c the concentrator field-of-view (FOV) semi-angle. Note that within the FOV of the PD, the concentrator gain is constant. Further, also the signal transmission gain can be modelled as a constant. Hence, we can rewrite the channel gain as

$$\alpha = \frac{\gamma}{d^2} \cos^m \phi_S \cos \phi_R, \quad \text{for } \phi_R \le \psi_c,$$

(7)

where the prefactor $\gamma = \frac{(m+1)A}{2\pi} T(\phi_R) g(\phi_R)$ is constant for $\phi_R \le \psi_c$.

From (2) and (7), it follows that the RSS value depends on the distance d through the channel gain. This channel gain is in inverse proportion to d^2, but further depends on the distance and orientation through the angles ϕ_S and ϕ_R. In order to determine the relationship between ϕ_R, ϕ_S and d, we introduce two additional coordinate systems: (i) the LED-centric coordinate system (LCS) (x', y', z'), and (ii) the receiver-centric coordinate system (RCS) (x'', y'', z''). To obtain the relationship between the different coordinate systems, we define the orientations of the LED and PD through the Euler angles, i.e. for the LED, we have the Euler angles set $\boldsymbol{\psi}_S = (\psi_{S,1}, \psi_{S,2}, \psi_{S,3})$, and for the PD the set $\boldsymbol{\psi}_R = (\psi_{R,1}, \psi_{R,2}, \psi_{R,3})$, where the first and third angle correspond to a rotation around the z-axis, and the second angle to a rotation around the y-axis. The LCS coordinates are obtained by applying the rotations $\boldsymbol{\psi}_S$ to the GCS coordinate system, with as center the LED with GCS coordinates $\mathbf{r}_S = (x_S, y_S, z_S)$:

$$\mathbf{r}' = \mathbf{M}_{\psi_{S,3}} \mathbf{M}_{\psi_{S,2}} \mathbf{M}_{\psi_{S,1}} (\mathbf{r} - \mathbf{r}_S),$$

(8)

where $\mathbf{r} = (x, y, z)$ are the coordinates in the GCS, and $\mathbf{r}'$ the coordinates in the LCS. It is clear that based on (8), $\mathbf{r}'_S = \mathbf{0}$. The rotation matrices are given by

$$\mathbf{M}_{\psi_{S,i}} = \begin{pmatrix} \cos \psi_{S,i} & \sin \psi_{S,i} & 0 \\ -\sin \psi_{S,i} & \cos \psi_{S,i} & 0 \\ 0 & 0 & 1 \end{pmatrix}, \quad i = 1, 3,$$

$$\mathbf{M}_{\psi_{S,2}} = \begin{pmatrix} \cos \psi_{S,2} & 0 & -\sin \psi_{S,2} \\ 0 & 1 & 0 \\ \sin \psi_{S,2} & 0 & \cos \psi_{S,2} \end{pmatrix}.$$

(9)

Similarly, the RCS coordinates are obtained by applying a rotation to the GCS, but now with as center the PD, having GCS coordinates $\mathbf{r}_R = (x_R, y_R, z_R)$:

$$\mathbf{r}'' = \mathbf{M}_{\psi_{R,3}} \mathbf{M}_{\psi_{R,2}} \mathbf{M}_{\psi_{R,1}} (\mathbf{r} - \mathbf{r}_R),$$

(10)

where $\mathbf{r}'' = (x'', y'', z'')$ are the coordinates in the RCS, and the transformation matrices $\mathbf{M}_{\psi_{R,i}}$ are defined similarly as (9). Here, $\mathbf{r}''_R = \mathbf{0}$ is valid. The angles $\psi_{S,i}$ and $\psi_{R,i}$ are chosen so that $\mathbf{u}_{z'} = \mathbf{n}_S$ and $\mathbf{u}_{z''} = \mathbf{n}_R$, where $\mathbf{u}_{z'}$ and $\mathbf{u}_{z''}$ are the unit vectors of the z' and the z''
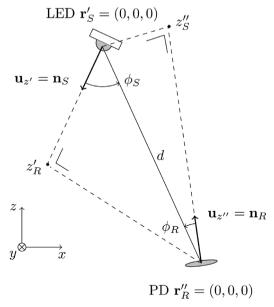

LED $\mathbf{r}'_S = (0, 0, 0)$

$\mathbf{u}_{z'} = \mathbf{n}_S$

ϕ_S

z''_S

z'_R

d

z

y

x

$\mathbf{u}_{z''} = \mathbf{n}_R$

ϕ_R

PD $\mathbf{r}''_R = (0, 0, 0)$

Fig. 2. Geometric interpretation of z'_R and z''_S.

axis, respectively. Let us denote z'_R as the z'-value of the receiver in the LCS coordinate system and z''_S as the z''-value of the LED in the RCS coordinate system. The geometric interpretation of z'_R and z''_S is shown in Fig. 2.

Using these coordinate systems, we can obtain the expressions for $\cos \phi_S$ and $\cos \phi_R$, corresponding to the definition of these angles in Fig. 1:

$$\cos \phi_S = \frac{z'_R}{d}$$
$$\cos \phi_R = \frac{z''_S}{d}.$$

(11)

where $d^2 = ||\mathbf{r}_S - \mathbf{r}_R||^2 = ||\mathbf{r}'_S - \mathbf{r}'_R||^2 = ||\mathbf{r}''_S - \mathbf{r}''_R||^2$. Note that, when $z'_R < 0$, the PD will not receive a signal as the LED does not radiate at angles ϕ_S outside the interval $[0°, 90°]$. Hence, $\alpha = 0$ if $z'_R < 0$. Further, when $z''_S < 0$, the LED will be out of the FOV of the PD. Hence, $\alpha = 0$ if $z''_S < 0$. Moreover, the concentrator gain is zero if $\phi_R > \psi_c$, which can be rewritten as $z''_S \geq d \cos \psi_c$. As the half-angle $\psi_c \in [0°, 90°]$, it follows that $d \cos \psi_c \geq 0$, which implies $z''_S \geq \max(0, d \cos \psi_c) = d \cos \psi_c$, i.e. the concentrator gain limits z''_S. Taking this into account, we obtain

$$\alpha = \gamma \frac{1}{d^{m+3}} (z'_R)^m (z''_S),$$

(12)

for $z'_R \geq 0$ and $z''_S \geq d \cos \psi_c$. The values z'_R and z''_S still depend on the distance d between the LED and the PD. Therefore, we take a closer look at these terms. First we recall that $\mathbf{r}'_S = \mathbf{0}$ and $\mathbf{r}''_R = \mathbf{0}$. Further, we denote $h = z_S - z_R$ as the vertical distance between the LED and the PD in the GCS, and $\Delta = h \tan \phi = \sqrt{d^2 - h^2}$ as the horizontal distance, and define the rotation angle φ:

$$x_S - x_R = \Delta \cos \varphi$$
$$y_S - y_R = \Delta \sin \varphi,$$

(13)

where ϕ and φ are defined as shown in Fig. 1. Elaborating (8) and (10) results in

$$z'_R = -\Delta \sin \psi_{S,2} \cos(\psi_{S,1} - \varphi) - h \cos \psi_{S,2}$$
$$z''_S = \Delta \sin \psi_{R,2} \cos(\psi_{R,1} - \varphi) + h \cos \psi_{R,2}.$$

(14)

To demonstrate the symmetry between the effects of the transmitter and receiver orientation and to simplify the interpretation of the results, we introduce the supplementary angle $\bar{\psi}_{S,2}$ of $\psi_{S,2}$ (i.e. $\bar{\psi}_{S,2} + \psi_{S,2} = 180°$).[1] The following expressions for z'_R and z''_S are obtained:

$$z'_R = -\Delta \sin \bar{\psi}_{S,2} \cos(\psi_{S,1} - \varphi) + h \cos \bar{\psi}_{S,2}$$
$$z''_S = \Delta \sin \psi_{R,2} \cos(\psi_{R,1} - \varphi) + h \cos \psi_{R,2}.$$

(15)

Hence, the condition $z'_R \geq 0$ can be rewritten as

$$\frac{\Delta}{h} \leq \frac{1}{\tan \bar{\psi}_{S,2} \cos(\psi_{S,1} - \varphi)}$$

(16)

and $z''_S \geq d \cos \psi_c$ as

$$\frac{\Delta}{h} \cos(\psi_{R,1} - \varphi) \geq \frac{d}{h} \frac{\cos \psi_c}{\sin \psi_{R,2}} - \frac{1}{\tan \psi_{R_2}},$$

(17)

which, depending on the sign of $\cos(\psi_{R,1} - \varphi)$, results in an upper or lower bound for Δ/h.

We notice that the channel gain, and thus the RSS value, is independent of the Euler angles $\psi_{S,3}$ and $\psi_{R,3}$. This is explained as follows. Recall that the distance d is independent of the considered coordinate system. Hence, the channel gain depends on the orientation of the LED and PD through their z-coordinates in the LCS and RCS only. As the last Euler angle corresponds to a rotation around the z-axis, it does not alter this z-coordinate. Therefore, without loss of generality, we can set $\psi_{S,3} = \psi_{R,3} = 0°$. In Fig. 3, the followed procedure for transforming the channel gain α is shown.

3. Planar distance estimation

3.1. Analysis

Under conditions (16) and (17), one can thus write down the value of the channel gain α that takes into account the tilting of the transmitter and receiver:

$$\alpha = \gamma \frac{(-\Delta \sin \bar{\psi}_{S,2} \cos(\psi_{S,1} - \varphi) + h \cos \bar{\psi}_{S,2})^m (\Delta \sin \psi_{R,2} \cos(\psi_{R,1} - \varphi) + h \cos \psi_{R,2})}{(\Delta^2 + h^2)^{\frac{m+3}{2}}}$$

(18)

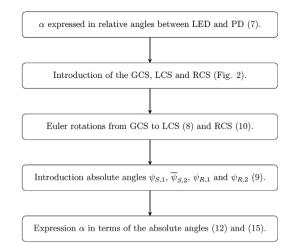[1] Remark that we work with angular degrees, where $180°$ corresponds with π radians.

Fig. 3. Flow chart summarizing the transformation of the channel gain α.

Obviously, when $\bar{\psi}_{S,2} = \psi_{R,2} = 0°$, the channel gain equals the well-known expression

$$\alpha_0 = \alpha|_{\bar{\psi}_{S,2}=\psi_{R,2}=0°} = \gamma \frac{h^{m+1}}{(\Delta^2 + h^2)^{\frac{m+3}{2}}} \tag{19}$$

Knowledge of α_0 (19) easily leads to a value of Δ since h is known. However, when we consider (18), finding an exact value for Δ with known parameters $\bar{\psi}_{S,2}$, $\psi_{R,2}$, $\psi_{R,1}$, $\psi_{S,1}$ and φ is clearly less straightforward. Nevertheless, by means of a numerical approach, determining the exact Δ still turns out to be feasible (e.g., we used the scipy.optimize.minimize [16] functionality for this purpose).

An interesting study is to evaluate the planar position estimation when it is erroneously supposed that both $\bar{\psi}_{S,2}$ and $\psi_{R,2}$ are perfectly equal to 0°, while in reality, this is not the case. When the receiver measures α when neither the transmitter nor the receiver are tilted ($\alpha = \alpha_0$), based on (19) and knowledge of h, we obtain the planar distance Δ by means of

$$\Delta^2 + h^2 = \left(\frac{\gamma h^{m+1}}{\alpha_0}\right)^{\frac{2}{m+3}} \tag{20}$$

Suppose however, that the user is not aware that the transmitter and/or receiver are tilted, and measures α from Eq. (18). Following the same procedure, the distance Δ will be estimated as $\hat{\Delta}$, where the following expression is valid:

$$\frac{\hat{\Delta}^2 + h^2}{\Delta^2 + h^2} = \left(\frac{\alpha_0}{\alpha}\right)^{\frac{2}{m+3}} = \left(\frac{h^{m+1}}{(z'_R)^m(z''_S)}\right)^{\frac{2}{m+3}} \tag{21}$$

Obviously, we are particularly interested in the planar position estimation error, defined as $\varepsilon_\Delta = \hat{\Delta} - \Delta$, that is being made for various tilt angles. Based on (21), this leads to

$$\varepsilon_\Delta = \sqrt{\left(\frac{h^{m+1}}{(z'_R)^m(z''_S)}\right)^{\frac{2}{m+3}}(\Delta^2 + h^2) - h^2} - \Delta \tag{22}$$

An interesting observation that can be made is that ε_Δ does not depend on the signal levels (note, noise is not included in the model) or γ, and is solely determined by the geometrical parameters and the order m of the Lambertian radiator. Secondly, it is observed that for $m = 1$, the importance of the receiver tilt (z''_S) is the same as the transmitter tilt (z'_R). For higher values of m (and thus more directive beams), the tilting of the transmitter has a higher weight in the overall planar position error than the receiver tilt. It is clear that ε_Δ is a value that depends on multiple parameters: Δ, φ, $\bar{\psi}_{S,2}$, $\psi_{S,1}$, $\psi_{R,2}$, $\psi_{R,1}$, h and m. In what follows, a procedure to reduce the complexity of the approach is elaborated, leading to a practical rule of thumb for the planar estimation error under receiver and/or transmitter tilt for various heights h and Lambertian orders m.

3.2. Numerical example

In this subsection, we will numerically determine the distribution of the planar offset ε_Δ for a representative set of tilting angles ($\bar{\psi}_{S,2}$ and $\psi_{R,2}$). We simulated the following configuration (see Fig. 1), where $x_S = y_S = 0$ and $z_S = h$, with h equal to 6 m, which is a representative value for larger facilities such as a warehouse. Initially, a value of $m = 1$ as Lambertian order of the transmitting LED is applied. In order to suppress the influence of the concentrator field-of-view semi-angle ψ_c, we have chosen this value equal to 90°. The receiver is positioned in the xy-plane ($z = 0$), with Δ varying between 0 and $+1.5h$ and φ between 0 and 360°. The location of the receiver is thus in a circular area with as center the xy position of the LED and radius 1.5h. A rotational symmetric observation area was chosen in correspondence with this property of the configuration. Remark that we did not consider any noise contribution, i.e.,
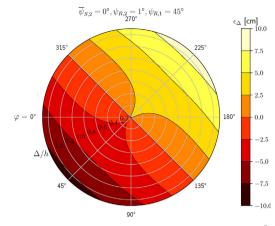
Fig. 4. The planar offset ε_Δ as function of $\Delta \leq 1.5h$ and $0 \leq \varphi < 360°$ for $h = 6$ m, $m = 1$, $\bar{\psi}_{S,2} = 0°$, $\psi_{R,2} = 1°$ and $\psi_{R,1} = 45°$.

the resulting bias values are completely due to the fact that tilting is not taken into account in the estimation process. Since $x_S = y_S = 0$ and taking into account (13), it is clear that the positive x-axis corresponds to $\varphi = 180°$ and the positive y-axis corresponds to $\varphi = 270°$.
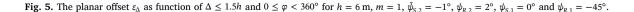
As a first configuration, we consider a receiver tilt $\psi_{R,2}$ of 1°, with $\psi_{R,1}$ equal to 45°, while there is no transmitter tilt ($\bar{\psi}_{S,2} = 0°$). This means that the receiver is directed to the LED when x and y are negative. Therefore, we expect that the planar distance will be underestimated in this third quadrant. The result is shown in Fig. 4, confirming the underestimation of the planar distance in the third and overestimation in the first quadrant. Another observation is that even a small tilting angle of 1° introduces position biases up to 10 cm, which is quite substantial, when the tilt effect is not taken into account. The value of $\psi_{R,1}$ is not critical here, since it only determines the direction of the receiver tilt.

In the second example, we focus on a configuration where we have a transmitter tilt $\bar{\psi}_{S,2}$ of − 1° and a receiver tilt $\psi_{R,2}$ of 2°, for some randomly chosen values of $\psi_{S,1}$ and $\psi_{R,1}$. When the user is not aware of the receiver ($\psi_{R,2}$) and transmitter tilt ($\bar{\psi}_{S,2}$), obviously, the direction ($\psi_{S,1}$ and $\psi_{R,1}$) of these tilting angles is also unknown. In Figs. 5–7, the distribution of the planar offset ε_Δ for identical tilting angles $\bar{\psi}_{S,2}$ and $\psi_{R,2}$, Lambertian order ($m = 1$) and height ($h = 6$ m) is shown. The range of errors clearly depends on the angles $\psi_{S,1}$ and $\psi_{R,1}$, which can be observed by considering the maximum values of ε_Δ.

3.3. Complexity reduction

When considering previous figures, it is clear that the distribution of the planar offset ε_Δ depends on a large set of parameters. In this subsection, we will, based on the sequential reduction of parameters, construct a simple and accurate rule-of-thumb, allowing the estimation of the planar position error when tilting is ignored.

The first step is to identify a single parameter for each distribution. Therefore, the expectation of $|\varepsilon_\Delta|$, known as the mean absolute error (MAE), is defined as in (23), with $\bar{\varepsilon}_\Delta$ expressed in cm.

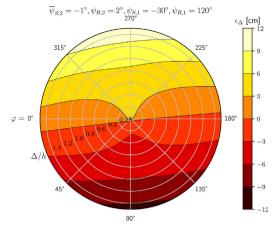$$\bar{\varepsilon}_\Delta = \mathbb{E}\{|\varepsilon_\Delta|\} = \frac{1}{S} \oint_{S=\{\Delta < 1.5h\}} |\varepsilon_\Delta| \, dS \tag{23}$$

Fig. 5. The planar offset ε_Δ as function of $\Delta \leq 1.5h$ and $0 \leq \varphi < 360°$ for $h = 6$ m, $m = 1$, $\bar{\psi}_{S,2} = -1°$, $\psi_{R,2} = 2°$, $\psi_{S,1} = 0°$ and $\psi_{R,1} = -45°$.

Fig. 6. The planar offset ε_Δ as function of $\Delta \leq 1.5h$ and $0 \leq \varphi < 360°$ for $h = 6$ m, $m = 1$, $\bar{\psi}_{S,2} = -1°$, $\psi_{R,2} = 2°$, $\psi_{S,1} = -30°$ and $\psi_{R,1} = 120°$.

Fig. 7. The planar offset ε_Δ as function of $\Delta \leq 1.5h$ and $0 \leq \varphi < 360°$ for $h = 6$ m, $m = 1$, $\bar{\psi}_{S,2} = -1°$, $\psi_{R,2} = 2°$, $\psi_{S,1} = 60°$ and $\psi_{R,1} = 180°$.

Due to this receiver position surface integration, the parameter space is reduced (integration over Δ and φ), but the MAE $\bar{\varepsilon}_\Delta$ still depends on $\bar{\psi}_{S,2}$, $\psi_{R,2}$, $\psi_{S,1}$, $\psi_{R,1}$, h and m. Let us consider $\bar{\varepsilon}_\Delta$ as a function of h taking previous distributions of Figs. 5–7 as representative examples. The result is shown in Fig. 8. Remark that a height h of 0 m has no practical meaning but it is useful to include in the model in order to perform an accurate fitting. The trend suggests a linear dependency on h, with an offset equal to 0 m. This was mathematically confirmed: a linear least-squares regression leads to an interception with the h-axis at $h = 0$ m and a correlation coefficient of 1, and this for all possible tilting angles. Consequently, (24) is valid, where β is the slope of the linear dependency expressed in cm/m.
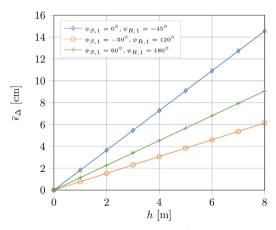

Fig. 8. The MAE $\bar{\varepsilon}_\Delta$ as function of h for the tilting angles $\bar{\psi}_{S,2} = -1°$ and $\psi_{R,2} = 2°$ of Figs. 5–7.
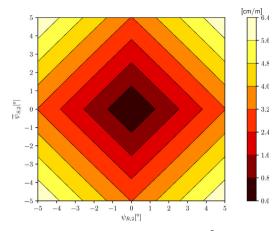
Fig. 9. The slope β_{max} as function of $\psi_{R,2}$ and $\bar{\psi}_{S,2}$ for $m = 1$.

$$\bar{\varepsilon}_\Delta(\bar{\psi}_{S,2}, \psi_{R,2}, \psi_{S,1}, \psi_{R,1}, m, h) = \beta(\bar{\psi}_{S,2}, \psi_{R,2}, \psi_{S,1}, \psi_{R,1}, m) \cdot h \tag{24}$$

Fig. 8 demonstrates that the slope value β strongly depends on $\psi_{S,1}$ and $\psi_{R,1}$. Therefore, for each value of $\bar{\psi}_{S,2}$ and $\psi_{R,2}$, we have determined the maximum value of β, called $\beta_{\max}$:

$$\beta_{\max}(\bar{\psi}_{S,2}, \psi_{R,2}, m) = \max_{\psi_{S,1}, \psi_{R,1}} \{\beta(\bar{\psi}_{S,2}, \psi_{R,2}, \psi_{S,1}, \psi_{R,1}, m)\} \tag{25}$$

$\beta_{\max}$ is the highest possible and thus worst-case slope, given the tilting angles $\psi_{R,2}$ and $\bar{\psi}_{S,2}$. In Fig. 9, the slope $\beta_{\max}$ is shown for $m = 1$. We performed a curve fitting on this distribution, and found

$$\beta_{\max}(\psi_{R,2}, \bar{\psi}_{S,2}, m = 1) \approx 0.633177(|\psi_{R,2}| + |\bar{\psi}_{S,2}|) \tag{26}$$

where $\beta_{\max}$ has the unit cm/m, with $\bar{\psi}_{S,2}$ and $\psi_{R,2}$ expressed in degrees. In Fig. 10, the difference between the numerical obtained values and approximation (26) is shown. Remark that in Fig. 10, the distribution is expressed in mm/m. Clearly, the model is very accurate and can be used to assess $\beta_{\max}$ for various tilt angles.

Let us illustrate the usefulness of the model as described by (26). Suppose that the transmitter is tilted over $-1.5°$ and the receiver is tilted $1°$, where the height h equals 4 m. Applying (26) leads to a value for $\beta_{\max}(1°, -1.5°, 1)$ of approximately 1.583 cm/m. Considering a height h of 4 m, we find that the highest and thus worst-case mean absolute error in a circular plane right below the LED with radius of 6 m ($=1.5h$) is 6.33 cm. By means of (26), assessment of this value is straightforward.

The procedure can be extended for transmitters with $m \neq 1$. This is illustrated in Fig. 11, where the distribution $\beta_{\max}(\psi_{R,2}, \bar{\psi}_{S,2})$ is shown for $m = 2$. Clearly, the interchangeability of $\psi_{R,2}$ and $\bar{\psi}_{S,2}$ as in Fig. 9 is no longer applicable. This is easily explained by relationship (20), where for $m \neq 1$, the symmetry between z'_R and z''_S is broken. As a consequence, relationship (26) can be generalized by

$$\beta_{\max}(\psi_{R,2}, \bar{\psi}_{S,2}, m = 1) \approx a|\psi_{R,2}| + b|\bar{\psi}_{S,2}| \tag{27}$$

where the expansion coefficients a and b are expressed in cm/($°$ m). In Table 1, these coefficients are shown. One clearly sees that the value of b, thus the importance of the transmitter tilt increases when the Lambertian order m becomes larger, fully in correspondence
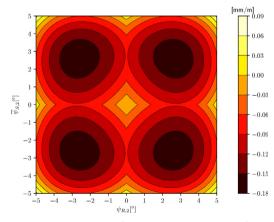

Fig. 10. $\beta_{max} - 0.633177(|\psi_{R,2}| + |\bar{\psi}_{S,2}|)$ as function of $\psi_{R,2}$ and $\bar{\psi}_{S,2}$ for $m = 1$.
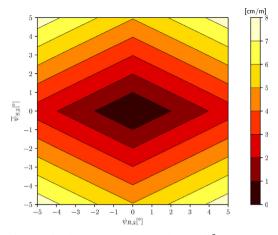
Fig. 11. The slope β_{max} as function of $\psi_{R,2}$ and $\bar{\psi}_{S,2}$ for $m = 2$.

Table 1
Table with summary of coefficients a and b (in cm/($^{\circ}$ m)).

Lambertian order m	a	b
1	0.633177	0.633177
2	0.507762	1.014544
3	0.422172	1.267048
4	0.361871	1.448418

to the mth power of z_R' in (21). With the coefficients as tabulated, a similar model accuracy as with $m = 1$ from Fig. 10 was obtained. To illustrate, when we take the same tilt angles as for the case $m = 1$, i.e. $\psi_{R,2} = 1°$ and $\bar{\psi}_{S,2} = -1.5°$, and height $h = 4$ m, we obtain for $m = 2$ a worst-case MAE of 8.12 cm, which is significantly higher compared to the $m = 1$ case.

4. Conclusions

In this work, we elaborated and applied general expressions for two-dimensional RSS-based visible light positioning solutions when tilting of the receiver and transmitter is applied. Of particular interest is the configuration where only small tilt angles occur, while the procedure to estimate the planar position neglects this tilt. It is demonstrated that the introduced position estimation bias depends solely on the geometrical parameters and the order of Lambertian radiator. Moreover, even when slight tilting occurs, values of more than 10 cm as bias are realistic. As a consequence, it is of utmost importance to take into account any possible tilting when accurate indoor positioning by means of RSS-based VLP is used, especially for configurations where the transmitting LEDs are attached to high ceilings such as in warehouse environments.

Analysis of the different configurations led to a useful and straightforward applicable rule-of-thumb that can be used for any height, allowing to determine the maximal mean absolute error when receiver and transmitting tilt are ignored.

Acknowledgements

References

[1] S. Bozkurt, A. Yazıcı, S. Günal, U. Yayan, A survey on RF mapping for indoor positioning, 2015 23rd Signal Processing and Communications Applications Conference (SIU) (2015) 2066–2069, https://doi.org/10.1109/SIU.2015.7130275.
[2] M.A. Al-Ammar, S. Alhadhrami, A. Al-Salman, A. Alarifi, H.S. Al-Khalifa, A. Alnafessah, M. Alsaleh, Comparative survey of indoor positioning technologies, techniques, and algorithms, 2014 International Conference on Cyberworlds (2014) 245–252, https://doi.org/10.1109/CW.2014.41.
[3] J. Armstrong, Y.A. Sekercioglu, A. Neild, Visible light positioning: a roadmap for international standardization, IEEE Commun. Mag. 51 (12) (2013) 68–73, https://doi.org/10.1109/MCOM.2013.6685759.
[4] Y. Zhuang, L. Hua, L. Qi, J. Yang, P. Cao, Y. Cao, Y. Wu, J. Thompson, H. Haas, A survey of positioning systems using visible led lights, IEEE Commun. Surv. Tutor. 20 (3) (2018) 1963–1988, https://doi.org/10.1109/COMST.2018.2806558.
[5] H. Steendam, T.Q. Wang, J. Armstrong, Theoretical lower bound for indoor visible light positioning using received signal strength measurements and an aperture-based receiver, J. Lightwave Technol. 35 (2) (2017) 309–319, https://doi.org/10.1109/JLT.2016.2645603.
[6] M.F. Keskin, S. Gezici, Comparative theoretical analysis of distance estimation in visible light positioning systems, J. Lightwave Technol. 34 (3) (2016) 854–865,

https://doi.org/10.1109/JLT.2015.2504130.

[7] M.F. Keskin, E. Gonendik, S. Gezici, Improved lower bounds for ranging in synchronous visible light positioning systems, J. Lightwave Technol. 34 (23) (2016) 5496–5504, https://doi.org/10.1109/JLT.2016.2620518.

[8] N. Stevens, H. Steendam, Magnitude of the distance estimation bias in received signal strength visible light positioning, IEEE Commun. Lett. 22 (11) (2018) 2250–2253, https://doi.org/10.1109/LCOMM.2018.2867026.

[9] S.D. Lausnay, L.D. Strycker, J. Goemaere, B. Nauwelaers, N. Stevens, A survey on multiple access visible light positioning, 2016 IEEE International Conference on Emerging Technologies and Innovative Business Practices for the Transformation of Societies (EmergiTech) (2016) 38–42, https://doi.org/10.1109/EmergiTech.2016.7737307.

[10] D. Plets, S. Bastiaens, L. Martens, W. Joseph, An analysis of the impact of led tilt on visible light positioning accuracy, Electronics 8 (4) (2019) 389, https://doi.org/10.3390/electronics8040389.

[11] E. Jeong, S. Yang, H. Kim, S. Han, Tilted receiver angle error compensated indoor positioning system based on visible light communication, Electron. Lett. 49 (14) (2013) 890–892, https://doi.org/10.1049/el.2013.1368.

[12] N. Stevens, H. Steendam, Influence of transmitter and receiver orientation on the channel gain for RSS ranging-based VLP, 2018 11th International Symposium on Communication Systems, Networks Digital Signal Processing (CSNDSP) (2018) 1–5, https://doi.org/10.1109/CSNDSP.2018.8471749.

[13] M.F. Keskin, S. Gezici, Comparative theoretical analysis of distance estimation in visible light positioning systems, J. Lightwave Technol. 34 (3) (2016) 854–865, https://doi.org/10.1109/JLT.2015.2504130.

[14] W. Raes, D. Plets, L. De Strycker, N. Stevens, Experimental evaluation of the precision of received signal strength based visible light positioning, 2018 11th International Symposium on Communication Systems, Networks Digital Signal Processing (CSNDSP) (2018) 1–4, https://doi.org/10.1109/CSNDSP.2018.8471827.

[15] J.M. Kahn, J.R. Barry, Wireless infrared communications, Proc. IEEE 85 (2) (1997) 265–298, https://doi.org/10.1109/5.554222.

[16] scipy.optimize.minimize, written by The SciPy community, (2018) (online; accessed 05.02.19), https://docs.scipy.org/doc/scipy/reference/generated/scipy.optimize.minimize.html#scipy.optimize.minimize.